HHS Public Access

Author manuscript

Nat Microbiol. Author manuscript; available in PMC 2020 November 18.

Published in final edited form as:

Nat Microbiol. 2020 August ; 5(8): 1011–1015. doi:10.1038/s41564-020-0725-x.

Lysogenic host-virus interactions in SAR11 marine bacteria

Robert M. Morris[1,†,*], **Kelsy R. Cain**[1,*], **Kelli L. Hvorecny**[2], **Justin M. Kollman**[2]

[1]School of Oceanography, University of Washington, Seattle WA 98195

[2]Department of Biochemistry, University of Washington, Seattle WA 98195

Abstract

Host-virus interactions structure microbial communities, drive biogeochemical cycles, and enhance genetic diversity in nature[1,2]. Hypotheses proposed to explain the range of interactions that mediate these processes often invoke lysogeny[3–6], a latent infection strategy used by temperate bacterial viruses to replicate in host cells until an induction event triggers the production and lytic release of free viruses. Most cultured bacteria harbor temperate viruses in their genomes (prophage)[7]. The absence of prophages in cultures of the dominant lineages of marine bacteria has contributed to an ongoing debate over the ecological significance of lysogeny and other viral life strategies in nature[6,8–15]. Here we report the discovery of prophages in cultured SAR11, the ocean's most abundant clade of heterotrophic bacteria[16,17]. We show the concurrent production of cells and viruses, with enhanced virus production under carbon-limiting growth conditions. Evidence that related prophages are broadly distributed in the oceans suggests that similar interactions have contributed to the evolutionary success of SAR11 in nutrient limited systems.

The SAR11 clade is comprised of a diverse group of heterotrophic bacteria that dominate life in the oceans. They account for >10^{28} cells globally and are only outnumbered by viruses that infect them or other plankton[8,16]. The range of host-virus interactions that have contributed to the success of SAR11 and their viruses is largely unknown, mostly because cultured marine viruses are primarily identified by their ability to kill a host. Although about half of all marine bacteria have a prophage[18–21], these latent bacterial viruses have not been identified in the ocean's most abundant cultured bacterioplankton. We previously isolated SAR11 from the North Pacific Ocean to identify trophic interactions[22]. Here we report the discovery of prophages in marine SAR11 (strains NP1 and NP2) that produce free viruses throughout the bacterial growth cycle.

---

† Corresponding author .

*These authors contributed equally to this work

Author Contributions

These authors contributed equally: RMM and KRC. RMM led the research effort, advised KRC on all research activities, conducted direct cell and virus counts, and wrote the paper with support from KRC, KLH, and JMK. KRC isolated SAR11 strains NP1 and NP2, sequenced the genome of strain NP1, verified the PNP1 phage integration site, maintained cultures and conducted growth experiments as part of her undergraduate research thesis. JMK advised KLH and contributed to the interpretation of TEM and associated data. KLH prepared samples for TEM analyses, took image, and quantified virus and vesicle-like particle sizes.

Competing Interests

The authors declare no competing interests.

Comparative analyses of the complete 1.38 Mbp Pelagibacter sp. strain NP1 genome indicate that it is most closely related to the first cultured representative from the SAR11 clade, *Ca.* Pelagibacter ubique HTCC1062[23] (Fig. 1). The NP1 genome is 56,946 bp longer than the HTCC1062 genome and codes for 37 more proteins. The average nucleotide identity (ANIb) and *in silico* DNA-DNA hybridization (DDH) values for NP1 and HTCC1062 are 90 and 41%, which are below the 94 and 70% threshold values typically used for species classifications, respectively. We therefore propose the name *Candidatus* Pelagibacter giovannonii strain NP1 in recognition of Stephen Giovannoni's discovery of the SAR11 clade and important contributions[24–26].

The most notable difference between strain NP1 and previously cultured SAR11 is that it contains a prophage (herein Pelagibacter phage PNP1). The prophage was first identified in an anomalous 35 Kbp section of the genome with >3 fold higher sequence coverage (Extended Data Fig. 1). The full 35,831 bp phage genome codes for 54 proteins, including those involved in transcriptional regulation, termination, and virus assembly. The genome is flanked by 40 bp direct repeats, indicating the core sequence for site-specific recombination and formation of hybrid *attL* and *attR* sites from virus *attP* and host *attB* attachment sites (Fig. 1; Extended Data Fig. 2 and Extended Data Fig. 3). The 40 bp core sequence is located upstream of a phage tyrosine integrase and in the host is part of a $tRNA^{met}$(CAT) gene. Tyrosine integrases typically recognize core sequences 6–8 bp long and that are flanked by inverted repeats[27]. Evidence that the same core sequence exactly matches a $tRNA^{met}$(CAT) genes in the HTCC1062 genome and sequences in published metagenomic datasets (Extended Data Fig. 4) suggests that PNP1 can integrate into the genomes of diverse SAR11.

Temperate prophages produce virions by spontaneous prophage induction (SPI), which is a low-frequency event that occurs under ideal growth condition[5], or non-spontaneously when DNA damage or stress induces a prophage at much higher rates[28]. We identified high SPI under carbon-replete growth conditions, with a virus-to-host ratio that reached 0.84:1 (Fig. 2A). A second lysogenic strain of SAR11 (NP2) had a similar growth rate and produced a similar virus-to-host ratio (0.85:1). Attempts to induce PNP1 virus production with known inducing agents were unsuccessful and suggest that induction studies underestimate the number of prophages in the oceans (Fig. 2B). Notably, host abundance did not decline significantly under carbon-replete conditions, even as virus abundance increased. This is in contrast to many other host-virus interactions, in which high concentrations of viruses are produced by significant cell lysis.

The virus-to-host ratio increased significantly under carbon-deplete growth conditions, reaching15:1 in stationary growth phase (Fig. 2C). Virus-to-host ratios are typically 10:1 in the oceans, though deviations are common and have prompted considerable debate over the range of interactions that structure microbial communities in high and low nutrient marine ecosystems [9–15]. We grew NP1 in a higher background of viruses to test for re-infection and confirm that carbon limitation was the cause of non-spontaneous prophage induction (Extended Data Fig. 5). There was no significant difference between the growth rate or final cell density of cultures started with a virus-to-host ratio of either 10:1 or 1:1. This suggests that lysogenic host-virus interactions enhance marine virus production under nutrient

limiting conditions. We measured virus decay to more accurately estimate virus production (Fig. 2D). Our estimate suggests that up to 2.3% of infected NP1 cells lysed and released virions by SPI under carbon-replete growth conditions and that up to 30.6% of infected NP1 cells lysed and released virions by non-spontaneous prophage induction under carbon-deplete growth conditions. Our estimates for the number of cells lysed by SPI are significantly higher than for other lysogenic bacteria[29]. Evidence of a concurrent vertical and horizontal transmission strategy that resembles chronic infections[30] supports theoretical predictions of hybrid lytic-lysogenic life strategies in nature[31].

Transmission Electron Microscopy (TEM) images show that lysogenic SAR11 cultures produce short-tailed podoviruses that are similar in size and morphology to other Pelagibacter viruses[8] (Fig. 3, Extended Data Fig. 6). Strain NP1 produces viruses with 70.7 nm (± 2.3 nm) capsids and strain NP2 produces viruses with 102.7 nm (± 7.7 nm) capsids, suggesting that these are different prophages. We also identified elongated cell morphologies, budding cells, and 20–300 nm diameter particles (n = 162) resembling membrane vesicles in other bacteria (Extended Data Fig. 7)[32]. Budding and viral lysis are known mechanisms of vesicle formation in bacteria[32], [33, 34]. The growth rate of strain NP1 is much slower than the growth rate of HTCC1062 on the same media (0.21 ± 0.02 and 0.41 ± 0.01 d^{-1}, respectively)[22, 35]. This could be due to the metabolic cost of producing and releasing viruses and vesicles, for defense against a viral superinfection[36], or for spreading phage susceptibility to other SAR11[37].

We identified closely related phage genomes in a metagenomic study of marine viruses from the Mediterranean Sea[38] and from the North Pacific[39] (Fig. 4). Synteny between PNP1 and all phage sequences recovered from the environment is highly conserved around core genes. They have 40 bp core sequences adjacent to tyrosine integrases that match tRNA sequences in SAR11 and an uncultured Marine Group II Euryarchaeota[40] (Extended Data Fig. 4). Recent evidence of prophages in freshwater SAR11[41] and other temperate phages in marine SAR11[42] point to a mechanism capable of mediating significant horizontal gene transfer in the environment.

Hypotheses proposed to explain the roles of viruses in structuring microbial communities, driving biogeochemical cycles, and enhancing genetic diversity in nature have predicted a wide range of interactions[2,6,10,11]. We show that temperate phages in lysogenic SAR11 produce virions throughout the bacterial growth cycle, that virion production increases under carbon-deplete conditions, and that related prophages are broadly distributed in seawater. The discovery that lysogenic SAR11 continuously produce viruses, with enhanced production under carbon-limiting conditions, raises the possibility that prophage-mediated lateral gene transfer (transduction) has contributed to the high rates of recombination underlying the evolutionary success of SAR11 in nutrient limited systems.

Methods

Genome sequencing:

Cultures for genome sequencing were grown from a single starter culture in 8 1L polycarbonate bottles containing filtered seawater media amended with 10 μM

dimethylsulfoniopropionate (DMSP), 25 μM taurine, and 50 μM 2,3-dihydroxypropane-1-sulfonate (DHPS), at the *in-situ* temperature of 13 °C, and in the dark under aerobic growth conditions. Cells were collected on sterile 0.2-μm Supor 200 polyethersulfone filters in late exponential growth phase (1×10^6 cells/ml). DNA was extracted, combined, and purified using a single DNeasy PowerClean Pro cleanup column (MO Bio Laboratories, Carlsbad, CA, USA). A total of 0.36 μg of purified DNA was recovered and submitted to the University of Washington's Genome Science Department's Pacific Biosciences Services lab. A PacBio single-molecule real-time (SMRT) 10-kb library was constructed and sequenced using a single SMRT cell on the PacBio RS II platform. A total of 360,986 subreads were acquired, with an N_{50} value of 2,993 bp. Subreads shorter than 50 bp or with a quality score below 75 were removed prior to assembly. Initial *De novo* assembly of the genome from reads was conducted using the Hierarchical Genome Assembly Process 4 (HGAP4)[43]. Through the HGAP4 pipeline, reads were preassembled using BLASR, assembled using Celera, and polished using the Quiver consensus algorithm with default settings. The HGAP4 pipeline produced six linear contigs with a mean coverage of 697X. Another assembly was run using the Canu assembler version 1.2[44] to produce two linear contigs with overlapping ends and a mean coverage of 696X. Contigs produced by Canu were used as a reference for HGAP4 contigs. Gaps and ambiguous regions were sequenced by PCR using custom oligonucleotide primers designed using Geneious v11.1.5 (Biomatters, Auckland, NZ) and manufactured by Integrated DNA Technologies (Coralville, IA) (Extended Data Fig. 2). The final assembly produced a single linear contig with overlapping ends. Genome ends were aligned and trimmed in Geneious v11.1.5 to produce a single 1.38-Mbp circular chromosome. The complete, finished genome of strain NP1 was annotated using NCBI's Prokaryotic Annotation Pipeline. The exact location and orientation of the PNP1 prophage integration sites was determined by PCR analyses (Extended Data Fig. 2) of cultures in late stationary growth phase, which contained DNA sequences from the PNP1 prophage, free PNP1 phage, and strain NP1 bacteria without the PNP1 prophage. Genome sequences were aligned using the BLAST ringer generator Brigg[45] with sequences shared between strains NP1 and HTCC1062 set for >70% nucleotide sequence identity with an e-value cutoff of $\leq 1 \times 10^{-6}$.

Cultivation and growth experiments:

Ca. Pelagibacter giovannonii NP1 and Pelagibacter sp. strain NP2 were isolated from a dilution to extinction high-throughput cultivation experiment as previously described[22]. Briefly, bacteria from the deep chlorophyll maximum (40 m) in the North Pacific subpolar gyre (47°49.839' N, 129°44.990' W) were diluted to a final concentration of 1.76 cells mL^{-1} in filter sterilized seawater media supplemented with 20 μM DHPS. 1.7 milliliters of diluted cells were added to each well of an acid-washed and sterilized 96-well Teflon plate, then incubated in the dark at *in situ* temperature (13°C). Cell densities were determined every seven days for three weeks by staining with SYBR Green1 (Invitrogen, Eugene, OR, USA) and enumeration using an EasyCyte Plus Flow Cytometer (Millipore). Strain NP1 and NP2 were subsequently transferred into a modified artificial marine seawater media (AMS1), which was prepared using base salts, macronutrients, trace metals, and vitamins (Extended Data Fig. 8). The media did not include myo-inositol, 4-aminobenzoic acid, or organic buffers (HEPES or EDTA). The media was sparged overnight with filtered CO_2 and with air

to form a bicarbonate-based buffer. Carbon-replete media was prepared by adding 10 μM of DMSP, 25 μM DHPS, and 50 μM taurine. Carbon-deplete media consisted of modified AMS1, as noted above, with no additional carbon added. Growth experiments were carried out in 50 mL volumes in acid-washed and sterilized 250 mL polycarbonate bottles in biological triplicates. Culture identity and purity was verified before and after growth experiments by 16S rRNA sequence analysis. Prophage induction studies were conducted with 1 μg ml^{-1} of mitomycin C and 450 mW/cm^2 UV radiation for 30 seconds (Fig. 2).

Calculations:

The percentage of bacteria that lysed is V_t/42/B_t*100, where V_t is the total number of viruses and B_t is the total number of bacteria (Supplementary Data 1). We used 42 as an estimate of burst size because there are only minor differences in burst sizes for known SAR11 podoviruses (37, 42 and 49 $cell^{-1}$)[8]. PNP1 is most closely related to HTVC010P, which has a similarly sized genome, a slightly larger capsid, and a burst size of 42. We quantified virus decay using the equation $(1/t)*\ln(B_i/B_f)$ (Fig. 2D), were t is time, and B_i and B_f are the initial and final concentration of viruses, respectively.

Microscopy:

For epifluorescence microscopy, cells and viruses were filtered onto 0.02 μm pore size 25 mm Anodisc filters (Whatman), stained with SYBR Green I solution then fixed with Citifluor AF-1 antifade mounting solution (Ted Pela, Inc., Redding, Ca) as previously described[46]. Counts were determined for 10–20 images at each time point and for biological triplicates. Objects were differentiated by size (Extended Data Fig. 9). Virus abundance used to calculate the decay constant were measured in cultures that were 0.2 μm filter sterilized to remove cells. Bacterial growth was determined by quantifying cell abundance every 2 to 3 days using a flow cytometer[22]. Virus abundances and virus-to-host ratios were determined by counting cells and viruses weekly using a fluorescent microscope Negative stain transmission electron microscopy was used to image strain NP1 and NP2 cells and PNP1 and PNP1 phage particles. Cells and viruses were concentrated by ultracentrifugation and resuspension (64K RCF at 4 °C for 2 hours) or by centrifugal filtration (Amicon Ultra15). Cultures were applied to glow-discharged continuous carbon film grids in two ways: six microliters of culture were applied twice; or, cultures were ultracentrifugation directly onto grids (62.5K RCF at 4 °C for 1 hour). Grids were then washed in ddH_2O three times and negatively stained using 4% uranyl formate. Samples were imaged using a FEI Morgagni operating at 100 kV and a Gatan Orius CCD camera with the software package Digital Micrograph. Images were prepared in Fiji and assembled in Adobe Illustrator CC. A previous study found that only a small number of membrane vesicles were visible in seawater using the SYBR staining methods (average 0.01–0.1%)[34]. It is unlikely that the vesicle-like particles we identified by TEM impacted our direct virus counts.

Metagenomic sequence identification:

We identified viruses related to the PNP1 prophage in the subset of published metagenomic surveys that used long reads by searching the 40 bp direct repeat sequences identified in strain NP1 (*attB* site, tRNA-met CAT) and in PNP1 (*attP* site) against the nucleotide collection (nr/nt) using BLAST. Only identical matches were used for further analyses. We

then expanded the search using the first 40 bp of all tRNA sequences in *Ca.* P. giovannonii strain NP1. Identical matches were then aligned to the PNP1 prophage genome. For final confirmation, only complete phage genome sequences with a tyrosine integrase located directly adjacent to core 40 bp *attP* sequence that exactly matched a tRNA sequences in SAR11 were retained for further characterization (Fig. 4, Extended Data Fig. 4). It is likely that similar SAR11 prophages have gone undetected in short-read metagenomic surveys due to the inherent genetic complexity of SAR11 and marine phage[39]. PNP1-like prophages were identified in the subset of metagenomic surveys that sequenced complete virus genomes using fosmids or long-read sequencing.

Data Availability

Ca. P. giovannonii strain NP1 and associated data have been deposited under GenBank Accession Number CP038852 and BioProject number PRJNA531001. The strain NP1 16S rRNA sequence has been deposited under GenBank Accession number: MH923014. Original negative stain micrographs will be made available on request. *Ca.* P. giovannonii strain NP1 cultures have unique growth requirements and cannot be maintained in standard culture collections. Requests for bacterial cultures or DNA from the UW culture collection should be addressed to the corresponding author (RMM). Upon receiving of a request for materials, we will assist the requesting institution in completing a Uniform Biological Material Transfer Agreement. There is no transmittal fee for academic institutions.

Code Availability

No custom code was used in this study.

Extended Data

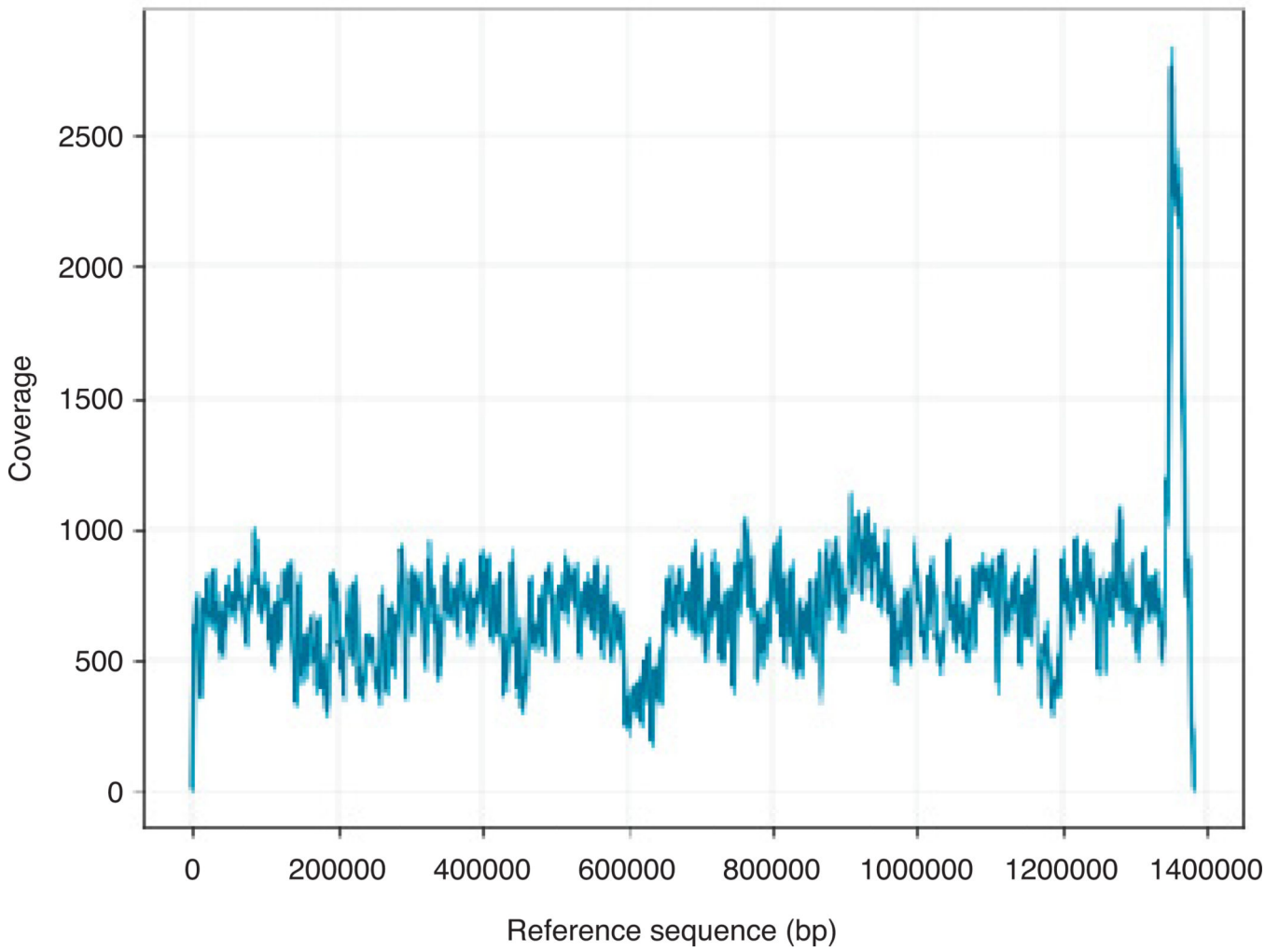

Extended Data Figure 1. Sequence coverage across the *Ca*. P. Giovannonii strain NP1 genome.
A total of 5346 reads. Mean coverage is 696 with 0 missing bases.

	Primer set	Primer Sequence (5'-3')	Target site	Product size (bp)
Phage insertion and excision	1,325,178F	GTGGGTCACACGCAATGGAT	*attL*	1291
	1,326,468R	TAGATCTCCGCCTATGTCGGC		
	1,361,398F	TGCAACCAGGAACTCTAATGCTG	*attR*	1095
	1,362,492R	TGCTCATTCCAAGTACCTAAAAGA		
	34,890F	AGAGAAGCCTCCGAAAAGACCA	*attP*	2041
	1,110R	CATCCACCATTTAAGCAGCGGA		
	1,325,178F	GTGGGTCACACGCAATGGAT	*attB*	1484
	1,362,492R	TGCTCATTCCAAGTACCTAAAAGA		
	5,360F	TGACTTTTCCGAGACGAGACCA	Internal virus control	1411
	6,770R	CCAGATGCAGTTGTGGACCAAA		
Genome verification	1,365,465F	CTGCTGCACTTGCTGGAAAAAC	Contig gap	1040
	799R	TCTAGTGGAGCCTGCTGCAATA		
	921,065F	CAGGTTCATGGTGGTTATGGGT	Contig gap	1371
	922,435R	GGGGCTCCACCAAAATGAGTTA		
	921,860F	AATACCGATGGTGGGAGCAGTA	Contig gap	1560
	923,419R	CTCAGAACTTCCATGACCAGGC		
	922,696F	CAAACACAGAGGGCGCTATTGT	Contig gap	1494
	924,189R	TCTTTCTGCAGCAACATCCCAT		

Extended Data Figure 2. PCR primers used to amplify NP1 and PNP1 DNA.

PCR primers were designed to connect genomic contigs, to validate genomic assemblies, and to identify phage insertion sites.

A

attB – ACAATAATTTATTGGCGGGGTAGCTCAGTCGGTTAGAGCGCAGGACTCATAAGCCTGAGGTCAGTGGTTCGATTCCACTTCCCGCTACCA
attP – CCAAATGGTCATTGGCGGGGTAGCTCAGTCGGTTAGAGCGCAGGACTCATAATTTTTAACATCAATTCC
attL – ACAATAATTTATTGGCGGGGTAGCTCAGTCGGTTAGAGCGCAGGACTCATAATTTTTAACATCAATTCC
attR – ACCAAATGGTCATGGCGGGGTAGCTCAGTCGGTTAGAGCGCAGGACTCATAAGCCTGAGGTCAGTGGTTCGATTCCACTTCCCGCTACCA

B

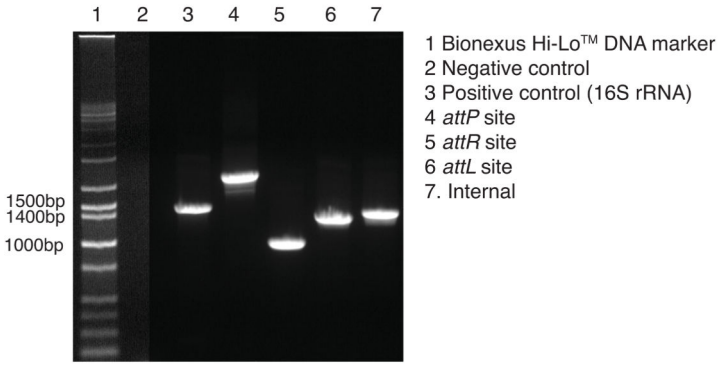

C

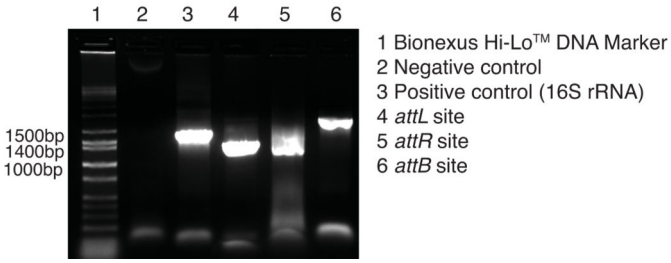

Extended Data Figure 3. Sequences associated with phage and host attachment sites verified by PCR.

A) The bacterial chromosomal sequence (*attB*), phage sequences (*attP*), and core sequences in blue, black, and red, respectively. B) PCR reactions verifying sequences associated with phage integration and excision, with bacterial (16S rRNA gene) and phage (internal) controls. All PCR products were sequenced to verify phage integration (*attL* and *attR* sites), a circular phage genome with an attachment site (*attP*), and phage excision from the bacterial chromosome with an attachment site (*attB*). PCR reactions were verified with DNA extracted from two or more cultures.

Source sequence (phage)	Match (host)	Accession
PNP1 (CP038852) TGGCGGGGTAGCTCAGTCGGTTAGAGCGCAGGACTCATAA	NP1	CP038852
	HTCC1062	CP000084
	Metagenomes	100+
Mediterranean phage (AP013398, AP013399, AP013385) ATTCCTCGGTAGCTCAGTTGGTAGAGCAGTTGACTGTTAA	NP1	CP038852
	HTCC1062	CP000084
	HIMB1321	LT840186
	HIMB5	CP003809
	RS 39	CP020777
	RS 40	CP020778
	Archaea	KF900592
	AFVG_250C00017	MK853003
	AFVG_250N00031	MK853017
	Metagenomes	100+
Mediterranean phage (AP013397) TGGGGGTGTAGCTCAGTTGGTTAGAGCGATCGCCTGTCAC	NP1	CP038852
	HTCC1062	CP000084
	HIMB1321	LT840186
	HIMB5	CP003809
	RS-39	CP020777
	FZCC0015	CP031125
	IOBCBE001	GQ234274
	Metagenomes	100+
North Pacific phage (MK853003, MK853017) ATTCCTCGGTAGCTCAGTTGGTAGAGCAGTTGACTGTTAA	NP1	CP038852
	HTCC1062	CP000084
	HIMB1321	LT840186
	HIMB5	CP003809
	RS-39	CP020777
	FZCC0015	CP031125
	IOBCBE001	GQ234274
	Metagenomes	100+

Extended Data Figure 4. Core PNP1 integration sequences identified in public databases.
40 bp core sequences identified in PNP1 (*attP*) and exact matches to tRNA sequences in SAR11 (*attB*) or to sequences in the NCBI genomic survey database.

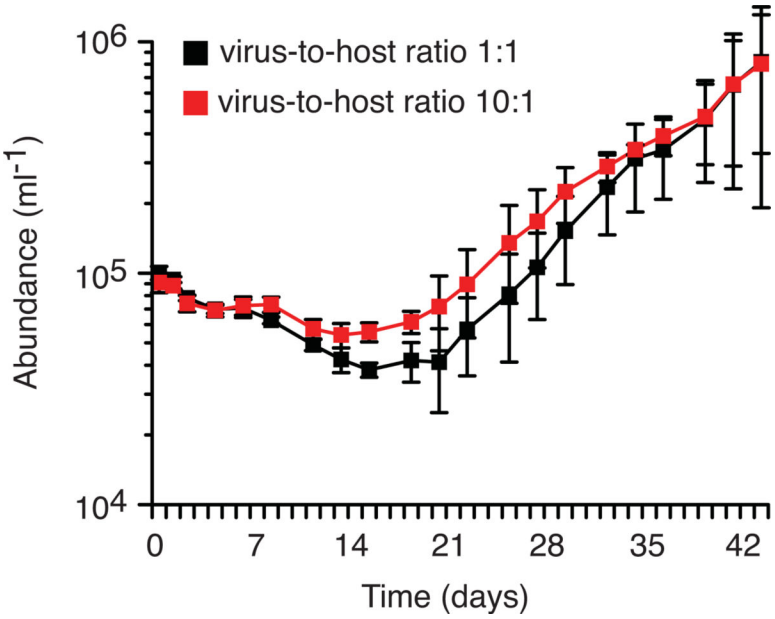

Extended Data Figure 5. *Ca.* P. Giovannonii strain NP1 growth initiated from cultures with PNP1 virions added at different ratios.

Ratio of 1:1 (black) and 10:1 (red). Data points are the mean of n=3 biologically independent samples and the error bars are the standard deviation.

Phage	Taxon	Capsid (nm ±)	Burst size (mean ±)	Genome size	G+C	Ref.
HTVC011P	Podoviridae	55 ± 2	49 ± 5	39,921	32.0	8
HTVC019P	Podoviridae	55 ± 1	37 ± 5	42,102	34.0	8
HTVC010P	Podoviridae	50 ± 3	42 ± 7	34,892	29.7	8
HTVC008M	Myoviridae	84 ± 3	9 ± 2	147,248	33.5	8
PNP1 (n=15)	Podoviridae	70.7 ± 2.3 (n=8)	ND	35,831	32.6	*
PNP2 (n=8)	Podoviridae	102.7 ± 7.7 (n=15)	ND	ND	ND	*

* This study

Extended Data Figure 6. Characteristics of PNP1 and PNP2.

Size and sequence characteristics of PNP1 and PNP2 phage relative to other Pelagibacter phages. Measurements are the mean from 2 independent biological samples of NP1 and 1 sample of NP2. Images were acquired from n=2–3 distinct regions on n=2–3 grids. Errors are the standard deviation.

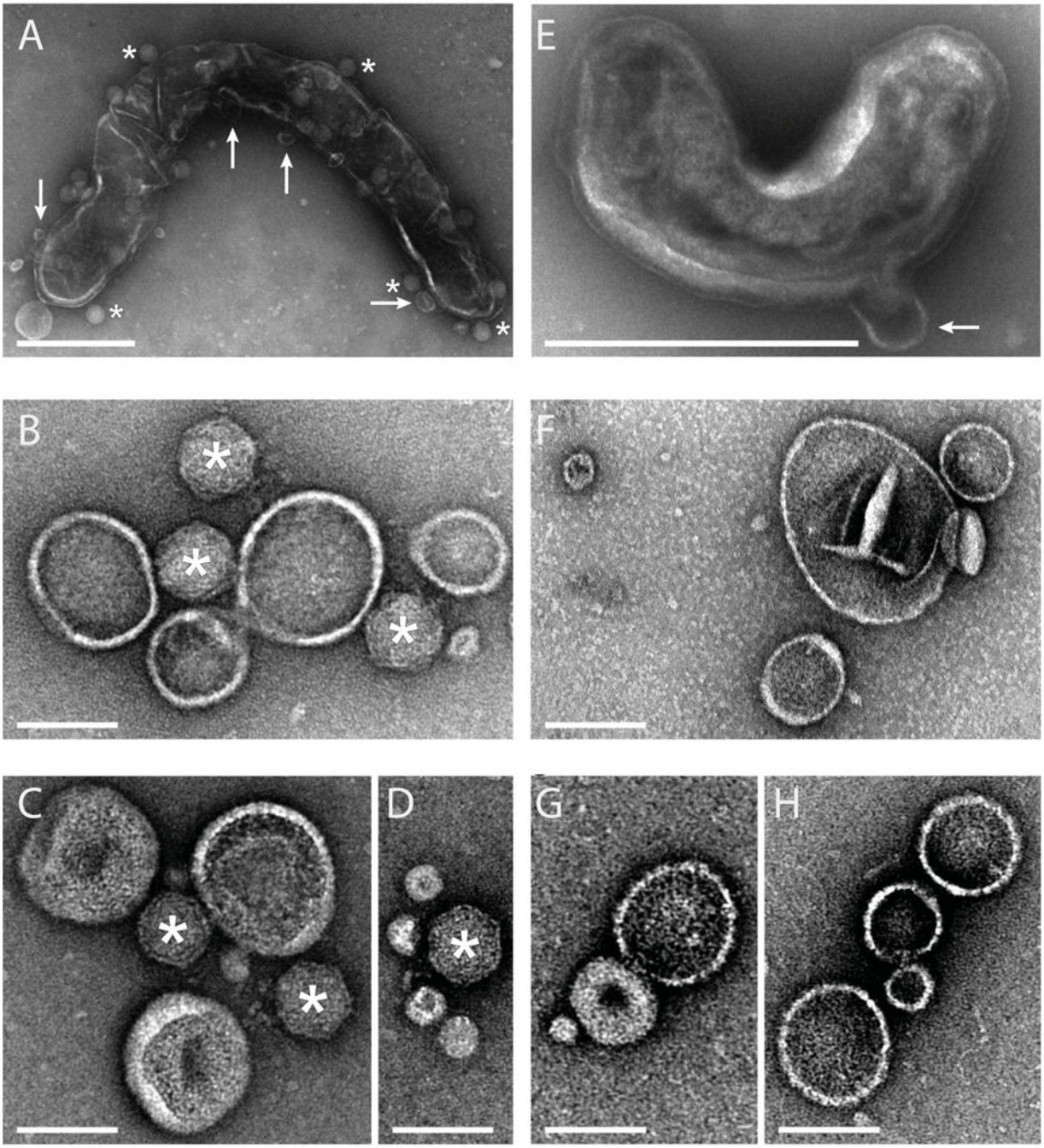

Extended Data Figure 7. Micrographs of strains NP1 and NP2, virions, and vesicle like particles.
A) Image of a *Ca.* P. giovannonii NP1 host cell with an elongated morphology, evidence of budding, and possible virion attachment. Image acquired at 8,900x. Arrow mark budding and asterisks mark virions; not all budding and viruses have been marked. B-D) Representative images of vesicle-like particles found in strain NP1, independently acquired at 22,000x; asterisks mark virions. E) Image of strain NP2 host cell showing evidence of budding, acquired at 14,000x. Arrow marks budding. F-H) Representative images of vesicle-like particles found in strain NP2, independently acquired at 22,000x. Scale Bars: A, E =

500 nm; B-D, F-H = 100 nm. Panels A-D, images from 2 separate cultures of NP1. Panels E-H, images from 1 culture of NP2. Images for cultures were acquired from 2–3 distinct regions on 2–3 grids.

Compound	Concentration
Salts	
NaCl	481 mM
$MgCl_2 \cdot 6H_2O$	27 mM
$CaCl_2 \cdot 2H_2O$	10 mM
KCl	9 mM
$NaHCO_3$	6 mM
$MgSO_4 \cdot 7H_2O$	2.8 mM
Macronutrients	
$(NH_4)_2SO_2$	400 μM
NaH_2PO_4 (pH 7.5)	50 μM
Trace metals	
$FeCl_3 \cdot 6H_2O$	117 nM
$MnCl_2 \cdot 4H_2O$	9 nM
$ZnSO_4 \cdot 7H_2O$	800 pM
$CoCl_2 \cdot 6H_2O$	500 pM
$Na_2MoO_4 \cdot 2H_2O$	300 pM
Na_2SeO_3	1 nM
$NiCl_2 \cdot 6H_2O$	1 nM
Vitamins	
B_1	6 μM
B_3	800 nm
B_5	425nm
B_6	500 nm
Biotin (B_7)	4 nM
B_9	4 nm
B_{12}	700 pM

Extended Data Figure 8. AMS1 base media.
Defined media used to grow SAR11 strain NP1 and strain NP2.

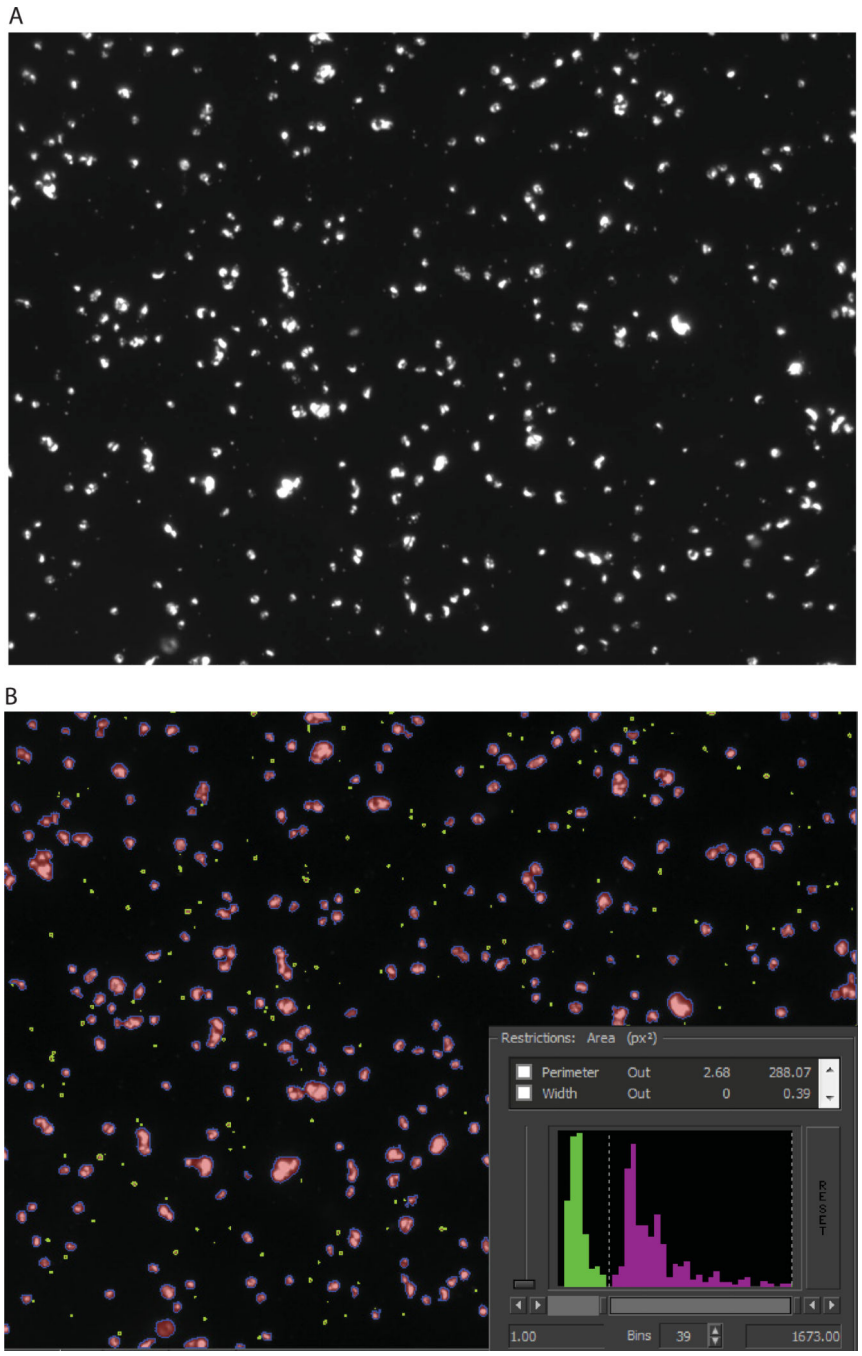

Extended Data Figure 9. Host and virus size exclusion of SYBR Green 1 stained particles.

A) Raw image of cells and free viruses stained, mounted, and viewed by epifluorescence microscopy. B) Cells (purple) and viruses (green) separated and enumerated by size exclusion (e.g. insert). All counts were determined by taking the average number of cells and viruses from 15–20 images at each time point and in biological triplicate. Direct cell and virus counts were repeated weekly on biologically independent samples and to verify continuous virus production in transfer cultures.

Supplementary Material

Refer to Web version on PubMed Central for supplementary material.

Acknowledgements

This work was funded by a grant from the National Science Foundation awarded to R. Morris and A. Ingalls (OCE-15584830). K.L.H. was support by the National Institute of Allergy and Infectious Disease, Award Number F32AI14511. We would like to thank members of the Center for Environmental Genomics at the University of Washington for their support and valuable feedback. We would especially like to thank Christina Rathwell for her valuable advice and thoughtful insights into marine virus ecology and Bryndan Durham and Mary Ann Moran for their help with experimental design leading to the cultivation of lysogenic strains of SAR11.

References

1. Rohwer F & Thurber RV Viruses manipulate the marine environment. Nature 459, 207 (2009). [PubMed: 19444207]
2. Breitbart M, Bonnain C, Malki K & Sawaya NA Phage puppet masters of the marine microbial realm. Nat. Microbiol. 3, 754–766 (2018). [PubMed: 29867096]
3. Stewart FM & Levin BR The population biology of bacterial viruses: why be temperate. Theor. Popul. Biol. 26, 93–117 (1984). [PubMed: 6484871]
4. Jiang S & Paul J Significance of lysogeny in the marine environment: studies with isolates and a model of lysogenic phage production. Microb. Ecol. 35, 235–243 (1998). [PubMed: 9569281]
5. Howard-Varona C, Hargreaves KR, Abedon ST & Sullivan MB Lysogeny in nature: mechanisms, impact and ecology of temperate phages. The ISME journal 11, 1511 (2017). [PubMed: 28291233]
6. Knowles B et al. Lytic to temperate switching of viral communities. Nature 531, 466 (2016). [PubMed: 26982729]
7. Kang HS et al. Prophage genomics reveals patterns in phage genome organization and replication. BioRxiv, 114819 (2017).
8. Zhao Y et al. Abundant SAR11 viruses in the ocean. Nature 494, 357 (2013). [PubMed: 23407494]
9. Våge S, Storesund JE & Thingstad TF SAR11 viruses and defensive host strains. Nature 499, E3 (2013). [PubMed: 23887434]
10. Giovannoni S, Temperton B & Zhao Y Giovannoni et al. reply. Nature 499, E4 (2013).
11. Thingstad TF & Bratbak G Microbial oceanography: viral strategies at sea. Nature 531, 454 (2016). [PubMed: 26982732]
12. Wigington CH et al. Re-examination of the relationship between marine virus and microbial cell abundances. Nature microbiology. 1, 15024 (2016).
13. Parikka KJ, Le Romancer M, Wauters N and Jacquet S Deciphering the virus-to-prokaryote ratio (VPR): insights into virus–host relationships in a variety of ecosystems. Biological reviews. 92, 1081–1100 (2017). [PubMed: 27113012]
14. Knowles B & Rohwer F Knowles & Rohwer reply. Nature 549, E3 (2017).
15. Weitz JS, Beckett SJ, Brum JR, Cael B & Dushoff J Lysis, lysogeny and virus–microbe ratios. Nature 549, E1 (2017).
16. Morris RM et al. SAR11 clade dominates ocean surface bacterioplankton communities. Nature 420, 806–810 (2002). [PubMed: 12490947]
17. Giovannoni SJ SAR11 bacteria: the most abundant plankton in the oceans. Annual review of marine science 9, 231–255 (2017).
18. Jiang SC & Paul JH Seasonal and diel abundance of viruses and occurrence of lysogeny/ bacteriocinogeny in the marine environment. Marine ecology progress series.Oldendorf 104, 163–172 (1994).
19. Jiang SC & Paul JH Occurrence of lysogenic bacteria in marine microbial communities as determined by prophage induction. Mar. Ecol. Prog. Ser. 142, 27–38 (1996).

20. Leitet C, Riemann L & Hagström Å Plasmids and prophages in Baltic Sea bacterioplankton isolates. J. Mar. Biol. Assoc. U. K. 86, 567–575 (2006).
21. Paul JH Prophages in marine bacteria: dangerous molecular time bombs or the key to survival in the seas? The ISME journal 2, 579 (2008). [PubMed: 18521076]
22. Durham BP et al. Sulfonate-based networks between eukaryotic phytoplankton and heterotrophic bacteria in the surface ocean. Nature Microbiology, 1 (2019).
23. Rappe MS, Connon SA, Vergin KL & Giovannoni SJ Cultivation of the ubiquitous SAR11 marine bacterioplankton clade. Nature 418, 630–633 (2002). [PubMed: 12167859]
24. Giovannoni SJ, Britschgi TB, Moyer CL & Field KG Genetic diversity in Sargasso Sea bacterioplankton. Nature 345, 60–63 (1990). [PubMed: 2330053]
25. Giovannoni SJ et al. Proteorhodopsin in the ubiquitous marine bacterium SAR11. Nature 438, 82–85 (2005). [PubMed: 16267553]
26. Giovannoni SJ et al. Genome streamlining in a cosmopolitan oceanic bacterium. Science 309, 1242–1245 (2005). [PubMed: 16109880]
27. Fogg PC, Colloms S, Rosser S, Stark M & Smith MC New applications for phage integrases. J. Mol. Biol. 426, 2703–2716 (2014). [PubMed: 24857859]
28. Ptashne M Principles of a switch. Nature chemical biology 7.8: 484 (2011). [PubMed: 21769089]
29. Owen SV et al. Characterization of the prophage repertoire of African Salmonella Typhimurium ST313 reveals high levels of spontaneous induction of novel phage BTP1. Frontiers in microbiology 8, 235 (2017). [PubMed: 28280485]
30. Hay ID & Lithgow T Filamentous phages: masters of a microbial sharing economy. EMBO Rep. (2019).
31. Weitz JS, Li G, Gulbudak H, Cortez MH & Whitaker RJ Viral invasion fitness across a continuum from lysis to latency. Virus evolution 5, vez006 (2019).
32. Toyofuku M, Nomura N & Eberl L Types and origins of bacterial membrane vesicles. Nature Reviews Microbiology. 17.1, 13–24 (2019). [PubMed: 30397270]
33. Biller SJ et al., Bacterial vesicles in marine ecosystems. Science 343,183–186 (2014). [PubMed: 24408433]
34. Biller SJ, McDaniel LD, Breitbart M, Rogers E, Paul JH and Chisholm SW Membrane vesicles in seawater: heterogeneous DNA content and implications for viral abundance estimates. The ISME journal 11, 394 (2017). [PubMed: 27824343]
35. Carini P, Steindler L, Beszteri S & Giovannoni SJ Nutrient requirements for growth of the extreme oligotroph ‘Candidatus Pelagibacter ubique’HTCC1062 on a defined medium. The ISME journal 7, 592 (2013). [PubMed: 23096402]
36. Bondy-Denomy J et al. Prophages mediate defense against phage infection through diverse mechanisms. The ISME journal 10, 2854 (2016). [PubMed: 27258950]
37. Ofir G and Sorek R Vesicles spread susceptibility to phages. Cell 168, 13–15. (2017) [PubMed: 28086086]
38. Mizuno CM, Rodriguez-Valera F, Kimes NE & Ghai R Expanding the marine virosphere using metagenomics. PLoS genetics 9, e1003987 (2013).
39. Beaulaurier J et al. Assembly-free single-molecule nanopore sequencing recovers complete virus genomes from natural microbial communities. bioRxiv, 619684. (2019).
40. Deschamps P, Zivanovic Y, Moreira D, Rodriguez-Valera F & López-García P Pangenome evidence for extensive interdomain horizontal transfer affecting lineage core and shell genes in uncultured planktonic thaumarchaeota and euryarchaeota. Genome biology and evolution 6, 1549–1563 (2014). [PubMed: 24923324]
41. Chen LX et al. Wide distribution of phage that infect freshwater SAR11 bacteria. bioRxiv, 672428 (2019).
42. Zhao Y et al. Pelagiphages in the Podoviridae family integrate into host genomes. Environ. Microbiol. 21, 1989–2001 (2019). [PubMed: 30474915]
43. Chin C et al. Nonhybrid, finished microbial genome assemblies from long-read SMRT sequencing data. Nature methods 10, 563 (2013). [PubMed: 23644548]

44. Koren S et al. Canu: scalable and accurate long-read assembly via adaptive k-mer weighting and repeat separation. Genome Res. 27, 722–736 (2017). [PubMed: 28298431]

45. Alikhan N, Petty NK, Zakour NLB & Beatson SA BLAST Ring Image Generator (BRIG): simple prokaryote genome comparisons. BMC Genomics 12, 1 (2011).

46. Noble RT & Fuhrman JA Use of SYBR Green I for rapid epifluorescence counts of marine viruses and bacteria. Aquat. Microb. Ecol. 14, 113–118 (1998).

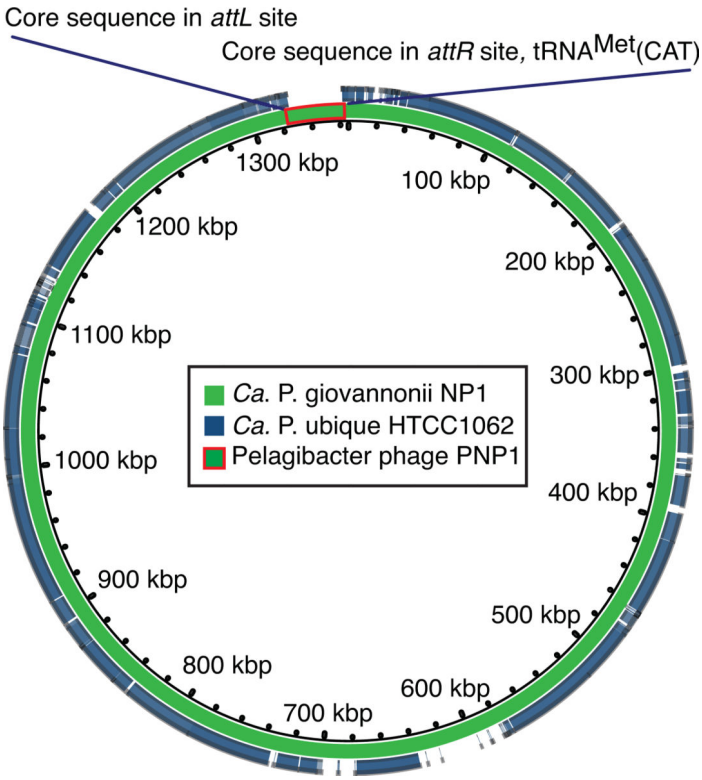

Figure 1.

Genome alignment of *Ca.* P. giovannonii strain NP1 to *Ca.* P. ubique HTCC1062. Inner ring, complete genome sequence of strain NP1 mapped to itself (green). Outer ring, complete genome of HTCC1062 (blue). Red border marks the location of the prophage. Black lines mark the location of the 40bp core nucleotide sequences (*attL* and *attR*) flanking the prophage genome.

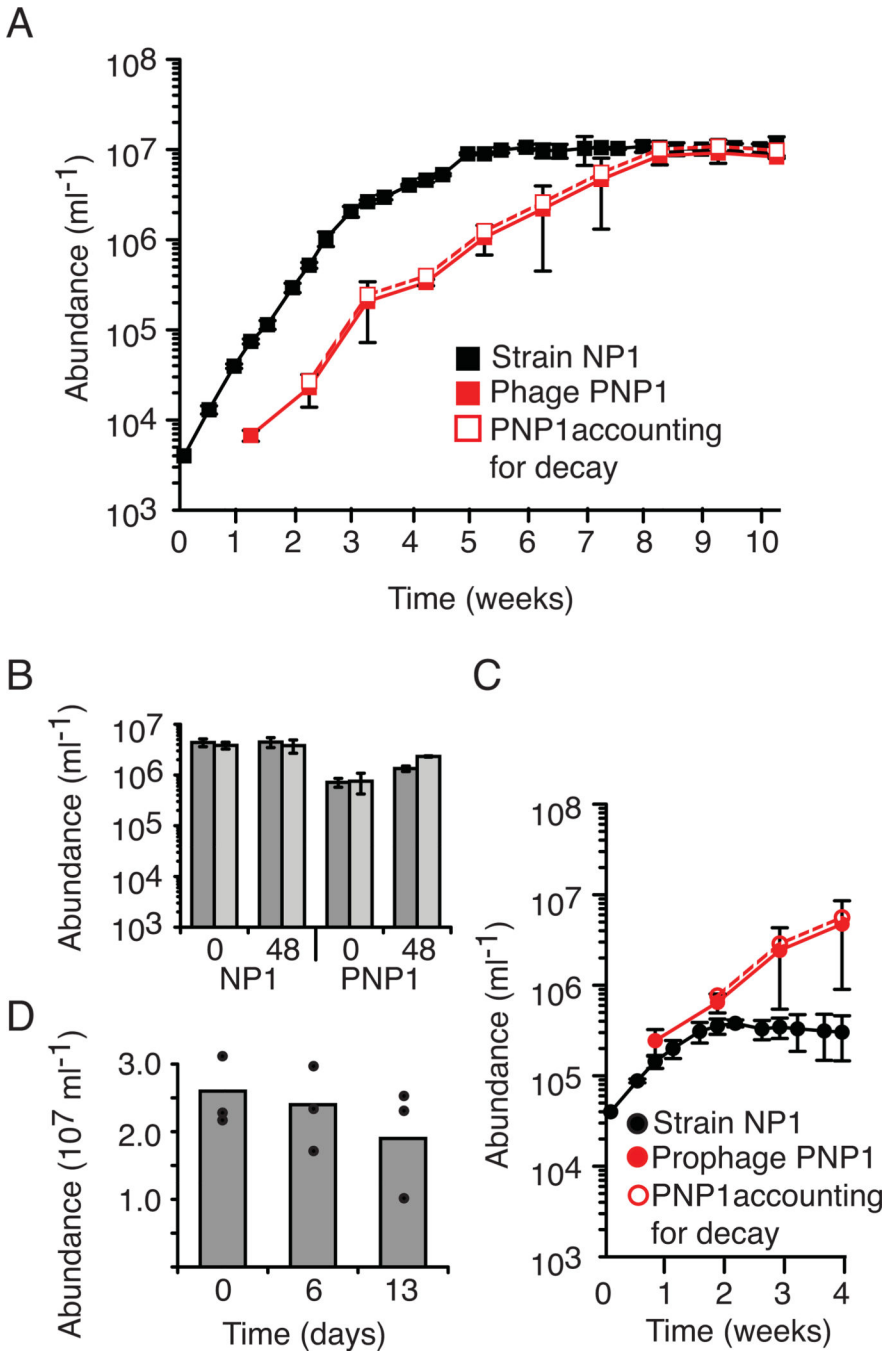

Figure 2.

Growth characteristics of *Ca.* P. giovannonii strain NP1 with phage PNP1. A,C) Strain NP1 growth and new virus production over the bacterial growth cycle on carbon-replete and carbon-deplete media, respectively. B) Prophage induction with mitomycin C (dark grey bars) and UV radiation (light grey bars). D) Virus decay over time in defined media. Data points in panels A-C are the mean of n=3 biologically independent samples and the error bars are the standard deviation. Bars in panel D are the mean of n=3 biologically

independent samples (dot plot). Evidence of concurrent bacterial and virus production was repeatedly verified in transfer cultures.

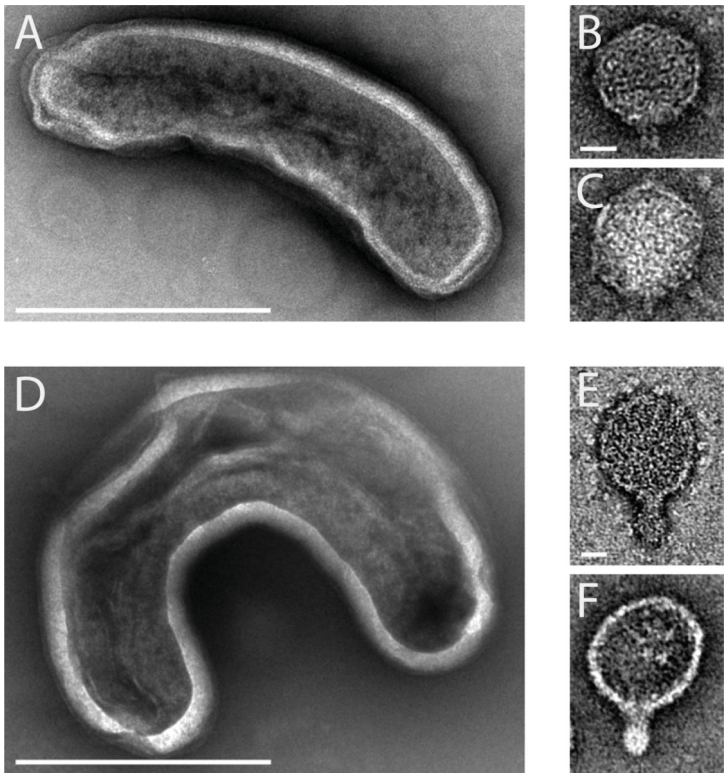

Figure 3.

Micrographs of *Ca.* P. spp. NP1 and NP2 and PNP1 and PNP2 virions. A) Image of a representative NP1 cell acquired at 14,000x. B,C) Images of PNP1 virions independently acquired at 44,000x. D) Image of NP2 cell acquired at 14,000x. E,F) Images of PNP2 virions independently acquired at 22,000x. Scale Bars: A, D = 500 nm; B, E = 25 nm. Panels A-C, cells and viruses from n=4 strain NP1 cultures. Panels D-F, cells and viruses from 1 culture of NP2. Images were acquired from n=2–3 individual regions on n=2–3 individual grids.

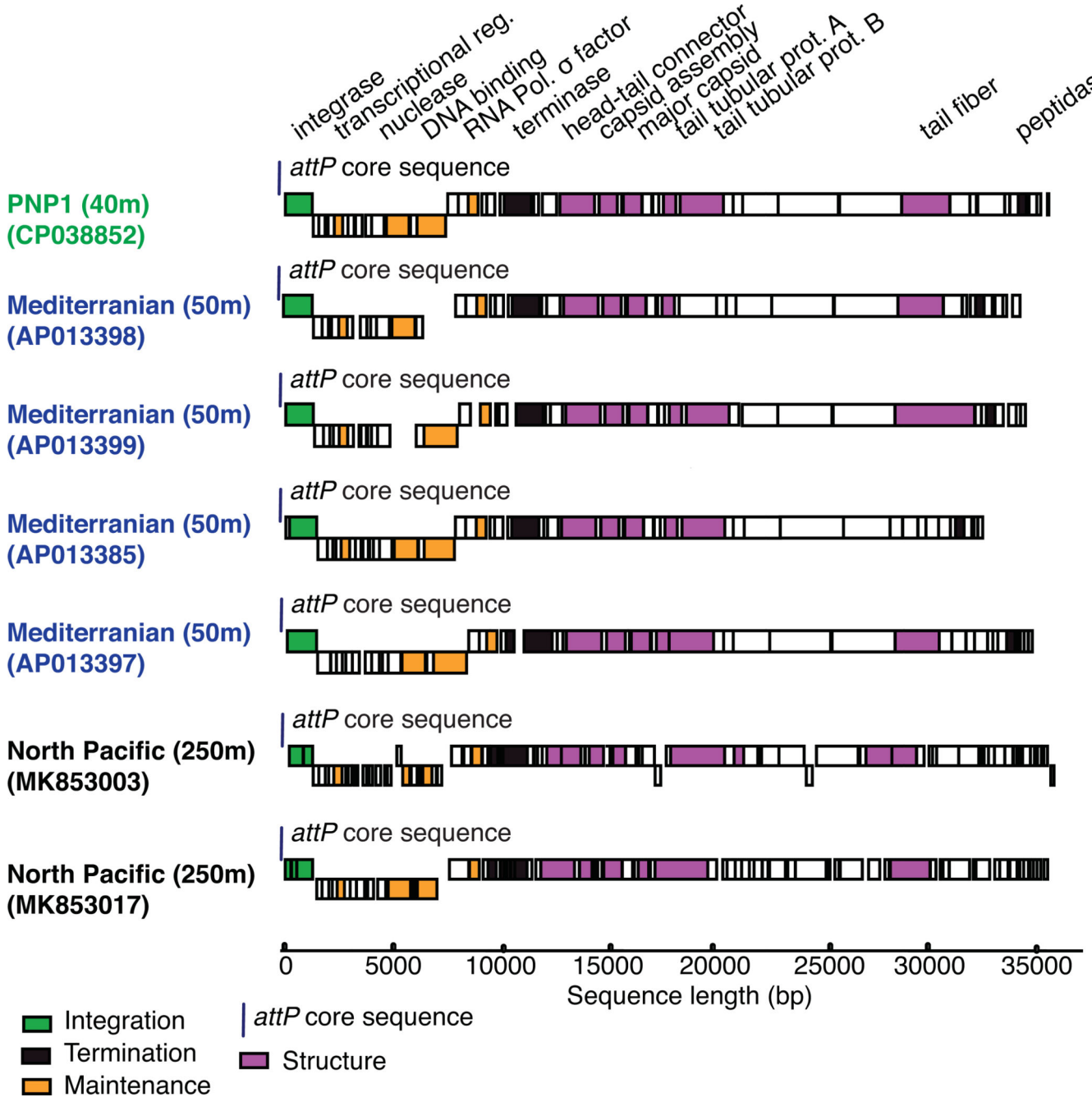

Figure 4.

Sequence alignment of PNP1 and related prophage recovered from seawater. Sequences derive from the Mediterranean Sea[37] and from 250 m in the North Pacific[38]. Black lines mark the location of 40bp core sequences associated with the *attP* site.